Chapter 5 : Pharmacokinetics of tg-FIX in the Factor IX-Knockout Mouse Hemophilia B Animal Model

5.1 Introduction

In the previous chapters, structural and *in vitro* functional properties of recombinant human FIX produced in transgenic pigs, tg-FIX, were ascertained. It was demonstrated that when expressed at 1-3 mg/ml, tg-FIX is composed of a mixture of post-translational modification (PTM) isoforms that can be fractionated into active and inactive populations by chromatographic methods. Even the most biologically active tg-FIX isoforms were shown to possess a unique PTM profile compared to plasma-derived FIX (pd-FIX). The circulating properties of proteins are often dependent upon their post-translational modifications, and as a result, any injected therapeutic protein, especially complex proteins produced in exogenous expression systems, must be assayed for *in vivo* survivability to determine their potential efficacy. To determine how the unique tg-FIX structure affects its potential function in treating hemophilia B, the circulating properties of tg-FIX *in vivo* must be investigated. A FIX product with full *in vitro* clotting activity is not viable if it is rapidly cleared or inactivated after injection.

Pharmacokinetics is the mathematical characterization of the time course of drug concentrations throughout the body. The pharmacokinetic properties of an infused drug are dependent upon its rate of elimination from plasma, including distribution of the drug from plasma to peripheral tissues and through drug clearance mechanisms. Due to their importance in determining dosage requirements, two pharmacokinetic properties are usually of most interest for a replacement FIX product: recovery and circulation half-life. Recovery is a measure of the increase in plasma concentration (IU/dl) per injected dose (IU/kg) and is most often defined from the highest measured plasma concentration of FIX within the first hour post-infusion.[1] It has been shown that after injection, FIX rapidly distributes to the vascular endothelium[2,3] and other tissues, most significantly the liver where close to 80% of injected FIX has been found within 2 minutes post-injection in mouse models.[4] It was initially thought that, due to its relatively low molecular weight, diffusion of FIX into interstitial fluids was also significant, but this has recently been

shown to be unlikely.[5] What FIX remains in plasma is then eliminated more slowly by as of yet unidentified clearance mechanisms.

It has been hypothesized that the circulating properties of FIX are dependent upon its post-translational processing.[6] This hypothesis was initially derived through the observation that recombinant FIX (rFIX) produced in Chinese hamster ovary (CHO) cells exhibits a lower *in vivo* recovery than plasma-derived FIX.[7] Another recombinant FIX, produced *in vitro* in human myotubes to test their potential efficacy in gene therapy, was also shown to possess a lower *in vivo* recovery than pd-FIX.[8] Though the primary amino acid sequence was identical, it was discovered that these rFIX preparations possess an altered post-translational modification (PTM) profile compared to pd-FIX. It was determined that this rFIX is incompletely sulfated at Tyr-155, with only 15% of rFIX sulfated compared to near 100% for pd-FIX, and it lacks the single phosphorylation of Ser-158 that is present in pd-FIX. Since this initial observation, it has been shown that pd-FIX can be transformed into a low-recovery species through de-phosphorylation and de-sulfation, further implicating these PTMs.[6] Additionally, it has been noted that infusion of rFIX enriched for sulfation exhibits a recovery similar to pd-FIX.[6] Interestingly, the lack of sulfation or phosphorylation has no effect on FIX clotting activity.[9]

Aside from the association of the phosphorylation and sulfation state with low *in vivo* recovery, little information is available on the effect of FIX PTMs on its pharmacokinetic profile. Despite its lower recovery, incompletely sulfated and phosphorylated rFIX exhibits an identical circulation half-life to pd-FIX.[9] The content and structure of N-linked oligosaccharides attached to circulating glycoproteins is often linked to plasma half-life,[10] though it has not been specifically implicated in this capacity for FIX. Certain glycoforms are known to be targeted for clearance in humans, including glycans possessing terminal galactose residues[10] (exposed by desialation of terminal sialic acids) and high-mannose glycans that are often present in recombinant proteins derived from yeast expression systems.[11] It is currently unknown if tg-FIX possesses either of these glycan structural elements.

In this study, pharmacokinetic properties of recombinant human FIX produced in the milk of transgenic pigs were investigated in factor IX gene knock-out mice (FIX-KO).

These mice are cross-reactive-material-negative (CRM^-),[12] as they possess no endogenous FIX to compete biologically with the administered FIX. Although cross-species FIX activity is not always observed, human FIX is functional in the murine coagulation system, capable of correcting FIX deficiency both *in vivo*[13,14] and *in vitro*.[16] Biologically active tg-FIX purified from transgenic pig milk was injected into FIX-KO mice and over a 72 hour time period after infusion of tg-FIX and pd-FIX, the plasma levels of active FIX were measured. It was found that tg-FIX exhibited a lower recovery, with a large percentage being eliminated from circulation rapidly after injection, but that circulating tg-FIX that survived the first 15 minutes potentially possessed a higher mean residence time and half-life. The observed differences in the pharmacokinetic profiles of tg-FIX and pd-FIX may be related to differences in post-translational processing. It was determined that tg-FIX has a lower Gla content, with an average of 7 Gla's compared to 11 for pd-FIX, which may affect the circulating characteristics of tg-FIX via altered endothelial cell binding.

5.2 Materials and Methods

5.2.1 Transgenic Milk Collection

Transgenic pigs were generated as and milk was collected as described previously.[18] Milk for these experiments was collected from pig K45 on day 43 of lactation, in which 2-3 mg FIX was expressed per ml of milk.

5.2.2 Preparation of tg-FIX for Injection

FIX was purified from pig milk using a combination of heparin-affinity and Q ion-exchange chromatography as described previously.[18] The high-salt elution fractions from multiple Mini Q columns were pooled and concentrated in YM-10 (10,000 MWCO) Centricon centrifugal concentrators (Millipore, Billerica, MA). The samples were concentrated by centrifugation using a constant angle rotor @ 1500 x g (3700 rpm, 10 cm radius) at 4°C. After the samples had been reduced to a volume of ~200 µl, the buffer was exchanged by the addition 1 ml of tg-FIX formulation buffer containing 10 mM histidine, 260 mM glycine, 1% sucrose pH 7.2 followed by centrifugation. This process

was repeated 3 times to ensure complete buffer exchange. The concentrated and buffer-exchanged sample was recovered by inversion of the apparatus and centrifugation at 250 x g (1500 rpm, 10 cm radius). Samples were frozen at -70°C until ready for use.

5.2.3 FIX Activation by Factor XIa and PNGase Digestion

CHO cell-derived rFIX (BeneFIX®, Wyeth, Collegeville, PA), pd-FIX (Mononine®, ZL Behring, King of Prussia, PA), and tg-FIX were subjected to activation by factor XIa. FIX was activated at 37°C for 5 hours in Tris buffered saline (TBS) containing 5 mM $CaCl_2$ and 0.5 mM factor XIa (Haematological Technologies, Inc., Essex Junction, VT). To stop the reaction, the reaction volumes were brought up to 10 mM EDTA.

For N-linked glycan comparison analysis, FIX was subjected to enzymatic cleavage of N-linked glycans by PNGase F. FIX was first denatured by incubation at 100°C for 5 minutes in a solution containing 0.2 % SDS and 0.1 M dithiothreitol (DTT). PNGase F (New England Biolabs, Beverly, MA) was then added to the denatured FIX solution and incubated for 3 hours at 37°C. The reaction was stopped by addition of the sample to SDS PAGE sample buffer.

5.2.4 ***SDS PAGE and Western Blot***

All electrophoresis and immuno-blotting was performed as described previously.[18]

5.2.5 ***FIX Activity – aPTT Assay***

The *in vitro* aPTT clotting activity assay was used to determine FIX specific activity as before.[18]

5.2.6 ***Phosphate Content-ProQ Diamond Assay***

Samples were treated as outlined in the ProQ Diamond phosphoprotein blot staining kit (Molecular Probes, Eugene, OR). The treated samples were then subjected to SDS PAGE on NuPAGE 10% Bis-Tris gels (Invitrogen, Carlsbad, CA). Protein in the

gel was then transferred to PVDF membrane and stained according to the manufacturer's instructions. After staining, the blot was air dried and visualized on a UVP transilluminator at 302 nm. Image was photographed using a Polaroid GelCam with a #23A red filter and a ¼ second exposure time. Amount of protein loaded on gel is indicated in the associated figure caption.

5.2.7 Total Gla Analysis

Amino acid analysis was utilized to determine the average Gla content of the FIX preparations as previously described.[18]

5.2.8 Pharmacokinetic Analysis

Intravenous Treatment of FIX-KO Mice

Pharmacokinetic experiments in factor IX gene knockout mice were performed by Professor Paul Monahan at the University of North Carolina. Plasma FIX activity levels were followed for 72 hours after bolus injection of either 300 IU/kg of tg-FIX (n=8) or 100 IU/kg of the pd-FIX product Mononine® (n=7) into FIX-KO mice (C57BL/6J-F9 ^{tmlDws}).[15] At 0.25, 1, 4, 24, 48, and 72 hours, mouse plasma FIX activity levels were measured by the aPTT clotting assay as described previously.[19] Measured IU/ml data was converted to percentage of normal FIX activity assuming 1 IU/ml as 100% FIX activity. At each timepoint, FIX activity is reported as an average of collected data points for all mice in the respective experimental group at that timepoint. FIX incremental recovery (defined as IU/dl rise in plasma per IU/kg administered) was calculated from the FIX activity measured in plasma at the first timepoint, 15 minutes, when FIX activity was the highest. The collected plasma concentration data was subjected to pharmacokinetic analysis through both one and two-compartment pharmacokinetic models as well as a model-independent analysis. Description of these pharmacokinetic analysis methods were taken from Riviere.[20]

One-compartment Model Analysis

The one-compartment pharmacokinetic model, depicted in Figure 5-1, is derived from two major assumptions about the behavior of a drug in the body. The first

assumption is that the administered drug distributes instantly and evenly into the plasma. Here, plasma is modeled as a single homogenous compartment without dissemination to other tissues, analogous to a well mixed beaker.

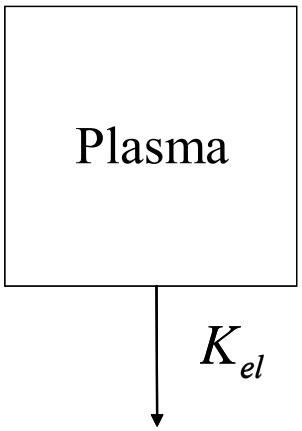

Figure 5-1. One-compartment pharmacokinetic model. After bolus injection, drug is distributed in homogenous single compartment (plasma) and eliminated by a first-order process defined by the elimination rate constant K_{el}.

The second major assumption of the one-compartment model is that the drug is eliminated from plasma at a rate that is proportional to its concentration, as described by equation 1, where Cp is the plasma concentration and K_{el} is the elimination rate constant.

$$\frac{dCp}{dt} = -K_{el}Cp \quad (1)$$

Through integration of equation 1, the plasma concentration of drug over time is represented by an exponential, equation 2.

$$Cp = Cp_o e^{-K_{el}t} \quad (2)$$

Equation 2 can be linearized by taking the natural logarithm of both sides and rearranging, shown in equation 3.

$$\ln Cp = \ln Cp_o - K_{el}t \quad (3)$$

A plot of ln(Cp) versus time yields a straight line of slope $-K_{el}$. The plasma half-life, the time at which $Cp/Cp_o = 0.5$, can then be calculated by plugging in the value for K_{el} obtained through linear regression of the plot obtained from equation 3.

$$t_{1/2} = \ln(2) / K_{el} \quad (4)$$

Both the major advantage and disadvantage of one-compartmental model analysis lie in its simplicity. The elimination rate constant as well as the plasma half-life can be easily calculated by linear regression of the semi-logarithmic plot of the plasma concentration profile. However, the simplicity of the model does not account for distribution of FIX from plasma to the vascular endothelium and peripheral tissues, as is thought to occur to a significant degree for FIX. As a result, the validity of the one-compartment model is questionable for this system.

For this analysis, the FIX concentration versus time data was plotted as ln(% Activity) versus time and linear regression of this plot was performed in Microsoft Excel to calculate K_{el} and C_{po}. The plasma half-life was then calculated by equation 4.

Two-Compartment Model

The two-compartment pharmacokinetic model represents a more complex treatment of the behavior of a drug in the body. As shown in Figure 5-2, this model accounts for distribution of a drug in both the plasma (compartment 1) and peripheral tissues (compartment 2). This distribution is described by the micro-rate constants k_{12} and k_{21}, which denote movement of the drug to and from the peripheral compartment respectively. This model relies upon the assumptions that the rate of drug clearance is proportional to the drug concentration, first-order elimination, and that clearance occurs only from the central compartment, assumed to be plasma.

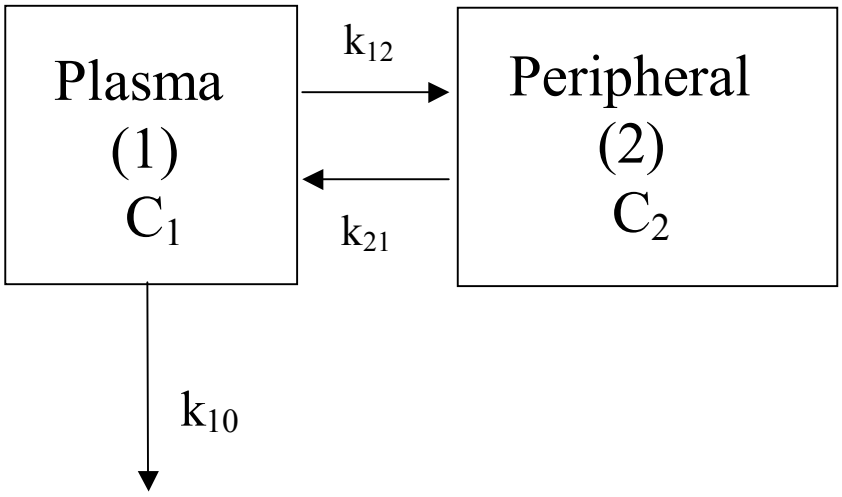

Figure 5-2. Two-compartment pharmacokinetic model. After bolus administration, the drug distributes in both the central compartment, plasma, and a peripheral compartment. The distribution is defined by the micro-rate constants k_{12} and k_{21}. The drug is cleared from plasma by a first-order process defined by the elimination rate constant, k_{10}.

From this model, drug distribution and clearance from the central and peripheral compartments are defined by the differential equations 5 and 6 respectively.

$$\frac{dC_1}{dt} = -(k_{12} + k_{10})C_1 + k_{21}C_2 \quad (5)$$

$$\frac{dC_2}{dt} = k_{12}C_1 - k_{21}C_2 \quad (6)$$

For the two-compartment system described in Figure 5-2 and equations 5 and 6, the plasma drug concentration versus time profile is a result of two separate processes: distribution of drug from plasma to the peripheral compartment and elimination of drug from plasma via clearance mechanisms. The plasma concentration over time, C_1, can be described by the sum of these two processes, each represented by an exponential, as shown in equation 7.

$$C_1 = A_1 e^{-\lambda_1 t} + A_2 e^{-\lambda_2 t} \quad (7)$$

By definition, the faster of the two processes is described by the first exponential with subscript 1. For FIX, distribution of FIX to peripheral tissues (compartment 2) occurs very rapidly and subsequently is described by the coefficients A_1 and λ_1. FIX elimination from plasma by clearance mechanisms is therefore described by coefficients A_2 and λ_2. These coefficients are related to the micro-rate constants k_{21}, k_{10}, and k_{12} by equations 8-10.

$$k_{21} = (A_1\lambda_2 + A_2\lambda_1)/(A_1 + A_2) \quad (8)$$

$$k_{10} = \lambda_1\lambda_2 / k_{21} \quad (9)$$

$$k_{12} = \lambda_1 + \lambda_2 - k_{21} - k_{10} \quad (10)$$

Each of the two processes, distribution and elimination, has a corresponding $t_{1/2}$, as described by equations 11 and 12.

$$t_{1/2}dist = \ln(2) / \lambda_1 \quad (11)$$

$$t_{1/2}el = \ln(2) / \lambda_2 \quad (12)$$

For this experiment, the plasma concentration versus time profile was fit to equation 7 by Mathcad using the *genfit* function which numerically fits a set of data to a user-defined equation. The micro-rate constants and half-lives were subsequently calculated from the resulting coefficients, $A_{1,2}$ and $\lambda_{1,2}$, by equations 8-12.

A statistical analysis was performed to determine if the bi-exponential equation derived from the two-compartment model represents a significantly better fit of the data than the one-compartment model mono-exponential equation. The F test compares the fit of two equations, where the equation with more parameters (in this case the bi-exponential equation) is a better fit (has a smaller residual sum of squares) than the equation with fewer parameters (the mono-exponential equation). The question to be answered in this analysis is whether the decrease in the residual sum of squares found

with the bi-exponential equation is worth the "cost" of the additional parameters (loss of degrees of freedom). The F statistic for this comparison is defined as follows:

$$F(\Delta df, df_{bi}) = \left(\frac{SS_{mono} - SS_{bi}}{SS_{bi}} \right) \cdot \left(\frac{df_{bi}}{df_{mono} - df_{bi}} \right) \quad (13)$$

In equation 13, SS_{mono} and SS_{bi} represent the residual sums of squares from both the mono-exponential and bi-exponential fits of the data while the terms df_{mono} and df_{bi} are the degrees of freedom associated with the two equations. Degrees of freedom are defined as the number of data points analyzed, in this case 5, minus the number of parameters in the fitted equation, 2 for the mono-exponential and 4 for the bi-exponential equation. The values for F calculated from the fits of both the tg-FIX and pd-FIX data were compared to the tabulated value for F of 199.5 (P = 0.05) given the values of the df. If the calculated F value was greater than 199.5, then the two-compartment model bi-exponential equation was accepted to provide a statistically significant better fit of the data.

Model-Independent Calculations

Model-independent pharmacokinetic analysis of the data was also performed. Model-independent calculations represent pure statistical analysis that operates under no assumptions about multiple compartments or the distribution of the drug in these compartments. Since plasma concentration is the measured variable, plasma is the only "compartment" that is considered. For model-independent calculations, the plasma concentration versus time function, Cp(t), is assumed to be a probability density function (pdf). The mean residence time (MRT) of a pdf is defined from statistical moment theory by equation 14, where, in pharmacokinetic studies, f(t) corresponds to the time-dependent plasma concentration Cp(t).

$$MRT = \frac{\int_0^\infty t \cdot f(t)dt}{\int_0^\infty f(t)dt} = \frac{AUMC}{AUC} \qquad (14)$$

The integral in the denominator is defined as area under the curve (AUC) and integral in the numerator is defined as area under the first moment curve (AUMC). MRT analysis was classically done by planimetry - plotting data and then cutting out the curves and weighing the paper. Another method is simply performing curve-fitting analysis to find the best equation to fit the data, and then integrating numerically or analytically.

Model-independent analysis for clotting factors offers advantages over the one and two-compartment models.[21] Primarily, model-independent analysis is not constrained by a mechanistic understanding of the processes of drug elimination and distribution. Though it is known that FIX does distribute to body tissues after injection, it is difficult to obtain biological data describing this distribution. Additionally, numerical integration of the AUC and AUMC plots can be easily performed without the need to use best-fit procedures to represent the data.

The model-independent MRT calculations were performed by evaluating the AUC and AUMC integrals by numerical integration techniques. Determination of the values for AUC and AUMC was first performed by directly analyzing the collected concentration versus time data. Here, imported pharmacokinetic functions for Microsoft Excel[22] which utilize the trapezoidal rule for integral calculation were used. Integration was performed either from t = 0 to t = 72 hours, or from t = 0 to t = ∞ assuming log-linear decline in plasma FIX concentration after the final collected timepoint, t = 72 hours. In addition to this analysis, curve fitting methods were utilized. Here, the plasma FIX concentration versus time data was curve fitted and then the resulting AUC and AUMC expressions were numerically integrated in Mathcad. The best and most realistic fits to the data were derived from one and two-term exponential equations, identical to those derived from the one and two-compartmental models. The half-life was then calculated from the resulting MRT values by:

$$t_{1/2} = \ln(2) \cdot (MRT) \quad (15)$$

5.3 Results

5.3.1 tg-FIX Product

Both the tg-FIX and pd-FIX products used in this study were checked for proteolytic degradation and activation by Western blot analysis (Figure 5-3). A significant quantity of activated FIX (FIXa), 10-20% of the total protein, is present in the tg-FIX preparation. FIXa migrates faster on SDS PAGE than single-chain zymogen FIX due to the removal of the activation peptide. Several other unidentified bands are also present in the tg-FIX preparation. The high MW bands likely represent aggregates of FIX, which also appear to a lesser extent in the pd-FIX preparation, while the low MW bands may correspond to FIX proteolytic products. By comparison, the majority of pd-FIX migrates as single-chain zymogen. The final tg-FIX product has a specific activity of 200 IU/mg as determined by the aPTT clotting assay.

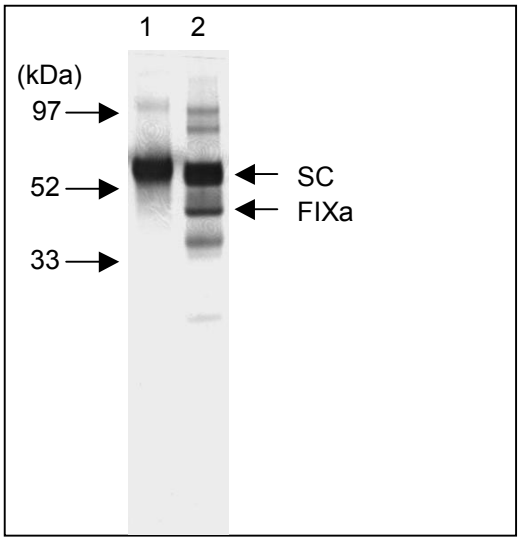

Figure 5-3. Western blot of FIX products. FIX products used in mouse injections, pd-FIX (Lane 1) and tg-FIX (Lane 2), were subjected to SDS PAGE under non-reducing conditions followed by Western blotting. Location of molecular weight standards are displayed as arrows on the left of the figure. Single chain FIX zymogen (SC) and activated FIX (FIXa) are indicated by arrows on the right.

5.3.2 Pharmacokinetic Analysis

After injection of a bolus of FIX into FIX-KO mice, FIX activity in mouse plasma was measured over a 72 hour time period via the aPTT clotting assay. The measured average plasma FIX activities are reported in Table 5-1, with the errors representing the standard deviation of the data. As shown in Table 5-2, the incremental recovery for tg-FIX, measured as IU/dl rise in activity per IU/kg injected, was much lower (approximately one-sixth) than pd-FIX. To ensure complete distribution, incremental recovery was measured 15 minutes after injection.

Time [hours]	tg-FIX at 300 U/kg dose %Activity in Plasma (n = 8)	pd-FIX at 100 U/kg %Activity in Plasma (n = 7)
0.25	33 ± 5 %	63 ± 15 %
1	21 ± 6 %	59 ± 7 %
4	20 ± 7 %	51 ± 22 %
48	6.0 ± 6 %	4.6 ± 5 %
72	4.3 ± 7 %	3.5 ± 2 %

Table 5-1. Measured FIX activities detected in mouse plasma after injection. tg-FIX (n=8) and pd-FIX (n=7) were injected into FIX-KO mice and the FIX activity in plasma was measured over time by the aPTT clotting assay. Reported activities are the average over the experimental groups. Errors represent the standard deviation of the collected data at each timepoint.

Factor IX IV Infusion	Incremental Recovery (IU/dl per IU/kg)
pd-FIX	0.63 ± 0.15
tg-FIX	0.11 ± 0.02

Table 5-2. Incremental recovery of FIX in FIX-KO mouse model**.** Incremental recovery for both pd-FIX and tg-FIX, measured as the IU/dl increase of FIX activity per IU/kg administered 15 minutes after injection, is reported here. Errors represent the standard deviation from the mean recovery.

One-Compartment Model

To derive a quantitative comparison of the circulating properties of tg-FIX and pd-FIX, the concentration versus time data was first analyzed by the simple one-compartment pharmacokinetic model. In this model, the concentration versus time profile is fit to a mono-exponential equation. In Figure 5-4, both the raw data the best-fit curve defined from the one-compartment model exponential equation are shown. The

data are fit reasonably well by this model, yielding R^2 values of 0.946 and 0.963 for the tg-FIX and pd-FIX data respectively. The circulation half-lives of tg-FIX and pd-FIX as calculated from this model are 27 and 16 hours respectively (Figure 5-5).

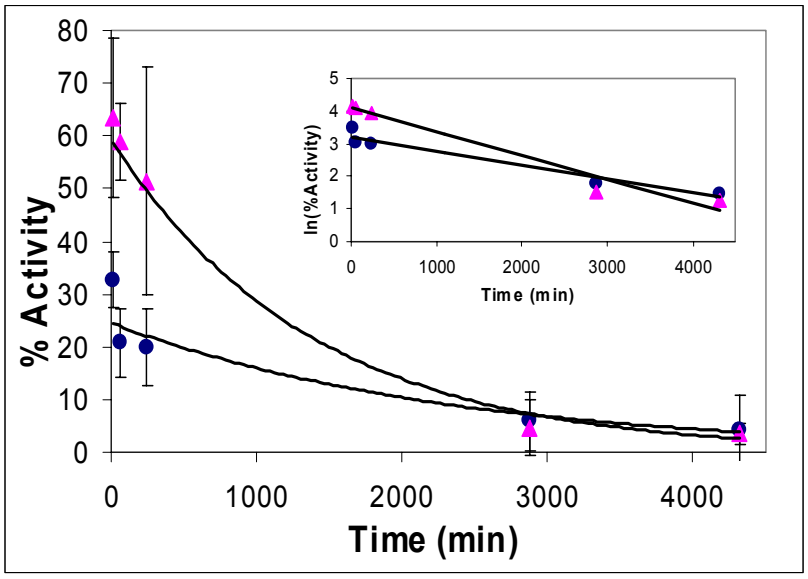

Figure 5-4. One-compartment model fit to concentration versus time data. Collected concentration versus time data for pd-FIX (▲) and tg-FIX (●) was fit to the exponential equation derived from the one-compartment model . Solid lines represent the one-compartment model exponential function utilizing K_{el} and C_{po} values derived from linearized plots of ln(%Activity) versus time (insert). Error bars represent the standard deviation of the measurements.

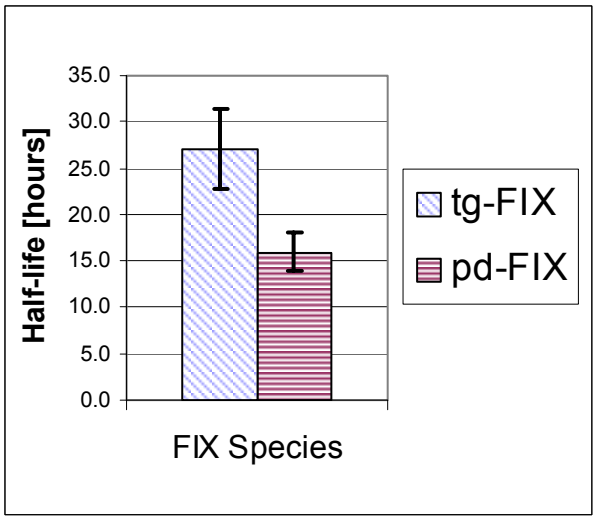

Figure 5-5. Half-life of tg-FIX and pd-FIX products calculated from the one-compartment model. The half-life of both pd-FIX and tg-FIX were calculated using one-compartmental analysis. Error bars represent the standard error of the slope from linear regression analysis.

Two-Compartment Model

Though the one-compartment model appears to represent a satisfactory fit to the data, the fit of the concentration versus time data to the two-compartment pharmacokinetic model was also investigated. This model is generally thought to provide a more accurate *in vivo* representation of FIX pharmacokinetics.[23,24] For the two-compartment model, the time-course profile of drug concentration is described by a bi-exponential equation, with one exponential representing rapid distribution of drug to peripheral tissues and the second the elimination of the drug from plasma via clearance mechanisms. The fit of the data by this model is shown in Figure 5-6. The two-term exponential equation fits the data very well, with all the residuals from the fit less than 2% of activity. From the two-term exponential equation coefficients derived from this fit, the micro-rate constants and both the distribution and elimination half-lives were calculated (Table 5-3). Of the micro-rate constants, only k_{21}, which physically represents the redistribution rate from the peripheral tissues to plasma, differs considerably between the two FIX products. The elimination half-life of tg-FIX as calculated from this model, 28 hours, is twice that of pd-FIX, 13.8 hours.

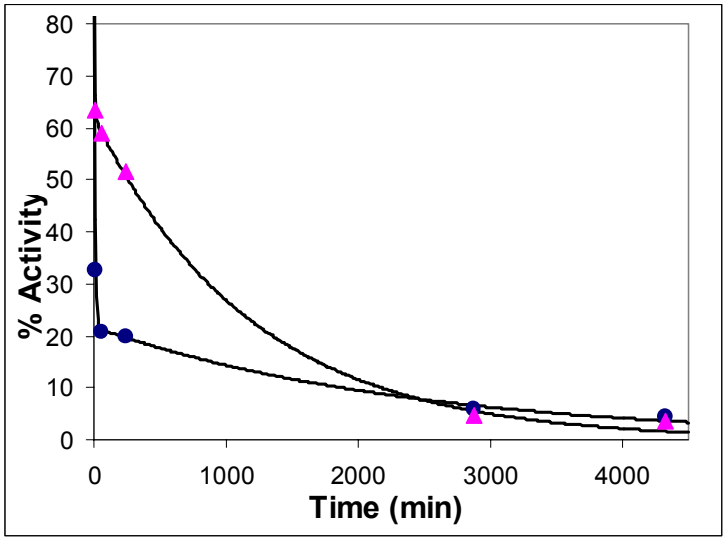

Figure 5-6. Two-compartment model fit to concentration versus time data. The pd-FIX (▲) and tg-FIX (●) data were curve fitted to the two-compartment model bi-exponential equation using Mathcad. Solid lines represent the best-fit curves to the data. Error bars of the standard deviation of the raw data were omitted..

	tg-FIX	pd-FIX
k_{12} (min^{-1})	0.091	0.087
k_{21} (min^{-1})	0.030	0.130
k_{10} (min^{-1})	0.0017	0.0014
$t_{1/2dist}$ (min)	5.7	3.2
$t_{1/2elim}$ (hr)	28	13.8

Table 5-3. Calculated two-compartment model parameters. The coefficients from the two-compartment model curve fits were used to determine the micro-rate constants and distribution and elimination half-lives of both tg-FIX and pd-FIX.

A statistical analysis (F-test) was performed to determine if the additional parameters introduced in the bi-exponential equation yield a statistically significant improvement in the fit of the data than the mono-exponential equation. From this analysis, F values of 3.8 and 33.0 were calculated by equation 13 for the pd-FIX and tg-FIX data fits respectively. Both of these values were less than the value of 199.0 required to meet achieve a 95% confidence level. As a result, though the two-compartment model is likely a more realistic depiction of the behavior of FIX *in vivo*, the data do not indicate this in a way that is statistically significant.

Model-Independent Analysis

As an alternative to the pharmacokinetic model analysis, the plasma FIX concentration versus time data were also analyzed by model-independent methods. This is a pure statistical analysis that assumes nothing about drug distribution into compartments and is often used in factor IX pharmacokinetic studies.[25,26] In this analysis, AUMC and AUC were determined by two different methods. The first was numerical integration in Mathcad utilizing the one and two-term exponential equations to estimate Cp(t). Other equations for fitting the concentration versus time profile were also investigated, including second and higher order polynomials, but they either yielded poor fits or were unrealistic representations of the data. For comparison, numerical evaluation of the AUC and AUMC by trapezoidal rule estimation utilizing the raw data was also

performed. The results from this analysis are shown in Table 5-4. Integration of the curve-fits yielded similar results for the half-lives and are close to the values reported for both the one and two-compartment model calculations. Integration using trapezoidal estimation, however, yielded somewhat lower values for MRT. This is most likely due to the endpoint estimation from t = 72 to infinity for the plasma concentration. In this analysis, after the last timepoint, a log-linear decline of FIX concentration was assumed to facilitate calculation.

Integration Method	MRT tg-FIX (Half-life)	MRT pd-FIX (Half-life)
Curve fit – One-term exponential	38.9 (27.0) hrs	23.0 (15.9) hrs
Curve fit – Two-term exponential	40.0 (27.7) hrs	19.8 (13.7) hrs
Data – Trapezoid: 0 to infinity	35.8 (24.8) hrs	14.3 (9.9) hrs

Table 5-4. Mean residence times (MRT) of tg-FIX and pd-FIX derived from the model-independent method using different integration techniques**.** The mean residence time of both tg-FIX and pd-FIX were determined by integration of the expressions for AUC and AUMC by the methods indicated. The half-life, calculated from the MRT, is shown in parentheses.

5.3.3 PTM Survey

It has been suggested that variations in the observed pharmacokinetic properties of FIX preparations in hemophiliacs are derived from altered post-translational modification.[6] In this study, it was found that the plasma recovery and circulation half-life of the tg-FIX and pd-FIX preparations differ significantly. In order to help explain these differences, the extent of post-translational processing of these preparations was assayed. The PTMs surveyed in this study include N-linked glycosylation, phosphorylation, and γ-carboxylation.

N-Linked Glycan Analysis

Plasma-derived FIX contains two N-linked glycans on the activation peptide.[27] To determine if tg-FIX possesses a similar N-glycosylation profile, digestion of the FIX preparations with PNGase, an endoglycosidase that cleaves only N-linked glycans,[28] was performed. Reduction in the apparent molecular weight of a N-glycosylated protein is

expected after PNGase digestion due to liberation of the glycan. CHO cell-derived rFIX, which possesses a similar glycosylation profile to pd-FIX,[29] was also assayed. As shown in Figure 5-7, the apparent molecular weight of the single-chain zymogen FIX form (SC) of all FIX preparations is reduced after PNGase digestion.

To localize the site of glycosylation, each FIX preparation was subsequently analyzed by a combination of factor XIa activation and PNGase digestion. Activation by factor XIa results in the proteolytic excision of the activation peptide, and when assayed on reducing SDS PAGE, activated FIX migrates as separate heavy chain, light chain, and activation peptide bands. The factor XIa activation products were subsequently digested with PNGase. It can be seen that the only species that exhibit an increased in migration velocity upon PNGase digestion are those containing the activation peptide. This includes single-chain zymogen FIX and the FIX heavy chain covalently attached to the activation peptide (HC+AP). The HC+AP FIX fragment is indicative of the presence of FIXα, a FIX activation intermediate that is cleaved only at the Arg^{145}-Ala^{146} bond. This FIXα intermediate represents a significant fraction of tg-FIX injected into the FIX-KO mice. These results indicate that the N-linked glycosylation sites of tg-FIX appear to be located on the activation peptide, similar to both pd-FIX and rFIX from CHO cells.

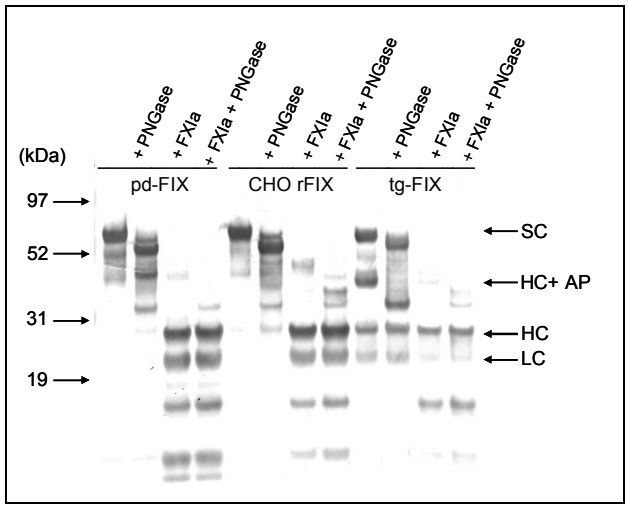

Figure 5-7. Western blot of PNGase digestions of FIX from different sources. pd-FIX, CHO cell derived rFIX, and tg-FIX were subjected to PNGase digestion (+PNGase) , activation by factor XIa (+FXIa), and PNGase digestion of factor XIa activation products (+FXIa +PNGase). Products were reduced (50 mM DTT) and run on SDS PAGE followed by Western blotting. The location FIX heavy chain (HC), FIX light chain (LC), heavy chain covalently attached to the activation peptide (HC+AP), and single chain zymogen FIX (SC) prior to PNGase digestion are indicated by arrows on the right of the figure. Location of molecular weight standards are indicated by arrows on the left of the figure.

Phosphorylation Analysis

Post-translational phosphorylation of Ser^{158} on the pd-FIX activation peptide has been implicated in plasma recovery[7] and may be important in determining other pharmacokinetic properties. Potential phosphorylation of tg-FIX was assayed using the ProQ Diamond phosphoprotein staining kit. As shown in Figure 5-8, both single-chain zymogen pd-FIX and tg-FIX are readily stained, indicating that both of these FIX preparations are phosphorylated. In the tg-FIX lane, another major band is visible, identified as HC+AP, that represents the FIXα activation intermediate. This intermediate was also detected in the Western blot of tg-FIX (Figure 5-7). The lower molecular weight bands observed in the tg-FIX sample are most likely highly phosphorylated caseins (abundant milk proteins) that were not completely removed from the tg-FIX sample. As a negative control, CHO cell rFIX, which lacks the Ser^{158} phosphorylation, was also assayed.

In order to localize the site of FIX phosphorylation to the heavy chain, light chain, or activation peptide, a sample of each of the three FIX preparations was activated by factor XIa and subjected to phosphorylation detection. In these samples, neither the tg-FIX heavy nor light chains were stained, indicating that the tg-FIX phosphorylation site

most likely located on the activation peptide, similar to pd-FIX. As further evidence of activation peptide phosphorylation, the HC+AP activation intermediate band of tg-FIX is stained. Interestingly, however, the released activation peptide from the factor XIa activations is not observed for either pd-FIX or tg-FIX. This peptide is consistently difficult to detect, as it is also not visible on SDS PAGE gels stained for total protein or Western blots probed with anti-FIX antisera.

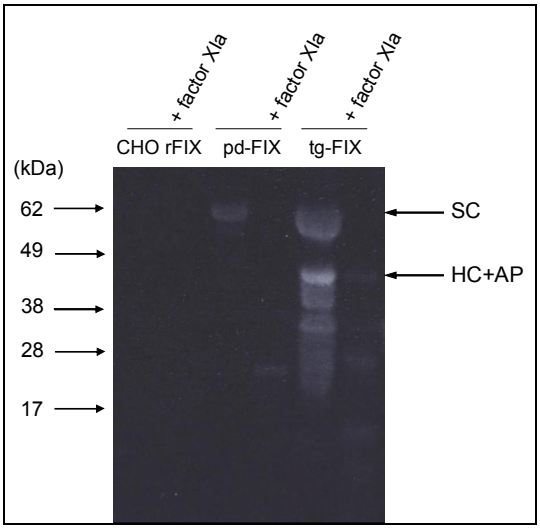

Figure 5-8. ProQ Diamond phoshoprotein-dependent staining of FIX. CHO cell-derived rFIX, pd-FIX, and tg-FIX both before and after activation by factor XIa (+factor XIa) were run on reducing SDS PAGE, transferred to PVDF, and then stained with a phosphoprotein-dependent staining method. The blot was then visualized in UV and photographed. Location of standard molecular weight markers are indicated on the left and the location of the proteolytic fragments are on the right. In the non-activated lanes, the maximum amount of protein was loaded to facilitate visualization: CHO rFIX/pd-FIX (7 μg) and tg-FIX (34 μg). All +factor XIa lanes contain 6 μg of total protein.

Gla Analysis

Both tg-FIX and pd-FIX were submitted for amino acid analysis to determine the average number of γ-carboxyglutamic acid residues (Gla's) per molecule. It was found that tg-FIX contained an average of 7 Gla's per molecule and pd-FIX contained 11. The 11 Gla's detected for pd-FIX is close to the expected 12 Gla's, demonstrating the accuracy of the amino acid analysis. Though low in Gla content, tg-FIX exhibits normal clotting activity. For this study, the other major FIX PTMs, O-linked glycosylation, tyrosine sulfation and β-hydroxylation of asparatate were not investigated.

5.4 Discussion

This research marks the first time that a recombinant FIX product derived from transgenic animals has been subjected to *in vivo* pharmacokinetic analysis. The goal of this study was to compare the pharmacokinetic properties of biologically active tg-FIX and pd-FIX in the hemophilia B mouse model. The hemophilia mouse model represents the first stage of preclinical testing for replacement FIX therapies due to the relatively low cost of maintaining mice compared to other animal models as well as the functional properties of human FIX in the murine blood coagulation system.

Upon injection into mice, FIX circulating behavior has typically been divided into two phases: rapid initial distribution of FIX to tissues, predominantly the liver, and endothelium,[24] and prolonged clearance of remaining circulating FIX. Incremental recovery is calculated as the maximum rise in plasma concentration of FIX per the administered dose. As a result, recovery of FIX is a function of both extent of distribution from plasma to peripheral tissues as well as any rapid initial clearance of FIX from circulation. In the FIX-KO mouse model, tg-FIX exhibited a very low plasma recovery, approximately one-sixth that of pd-FIX. From an economic and therapeutic standpoint this is problematic, as the amount of injected tg-FIX required to achieve 5% of normal circulating FIX levels necessary for normal hemostasis would be significantly greater than pd-FIX. This low recovery could be a consequence of two potential mechanisms: distribution of tg-FIX to peripheral tissues that occurs to a much greater extent than with pd-FIX or a rapid elimination pathway that specifically recognizes tg-FIX and not pd-FIX.

The most obvious potential cause for the low observed recovery of tg-FIX is the significant fraction of tg-FIX that has been converted to FIXa, as shown in Figure 5-3, which is susceptible to specific antithrombin III (ATIII)[4] and low-density lipoprotein receptor-related clearance pathways.[30] FIXa is rapidly bound *in vivo* by the serine protease inhibitor ATIII, inactivated, and removed from circulation by hepatocytes. Fuchs *et al.*[4] reported that the rate of FIXa inhibition by ATIII in mouse models is approximately 0.1 µg FIXa/ml plasma/min. Assuming 1.5 ml of mouse plasma, approximately 2.3 µg of FIXa would be inactivated by ATIII within 15 minutes. This 2.3 µg represents a significant percentage of the approximately 32 µg of FIX that was

injected. Because FIX activity levels (and not antigen levels) were measured, inactivated FIXa would not be detected in the measurement. Additionally, FIXa binds to the endocytotic low-density lipoprotein receptor-related protein (LRP). This receptor is present in various tissues (liver, lung, brain, and placenta) and cell types[31] and binds to a structurally variant spectrum of ligands, including the FIX cofactor factor VIII.[32] Ligand binding to LRP results in its transport from the cell surface to the endosomal degradation pathway. As a result, any FIXa injected as part of the tg-FIX preparation will be quickly cleared or inactivated through LRP-mediated degradation or ATIII inactivation, and reduce the observed recovery.

Additional tg-FIX may be susceptible to rapid elimination if either the ATIII or LRP clearance mechanisms recognize the FIX activation intermediate FIXα. FIXα is structurally and functionally distinct from both zymogen FIX and FIXa.[33] As shown in Figure 5-7, a significant fraction of FIXα was injected as part of the tg-FIX preparation. It has been shown that interaction of FIXα with ATIII differs from the ATIII/FIXa interaction. ATIII inhibits the amidolytic activity of both FIXa and FIXα in a 1:1 stoichiometric ratio, but, in contrast to the ATIII-FIXa complex, the interaction of ATIII with FIXα does not result in a SDS-resistant complex.[33] This indicates that the FIXα/ATIII interaction is not as strong as the interaction between FIXa and ATIII. Association of FIXa with LRP is mediated through an exposed surface loop, comprised of residues Phe^{342}-Asn^{346}, bordering the catalytic site on the FIXa heavy chain.[34] It is not known if the FIXα heavy chain contains a properly formed LRP binding site. However, the normal FIXa heavy chain catalytic site, adjacent to the area of LRP interaction, is only partially formed in FIXα.[33] Ultimately, it is unknown whether or not FIXα is cleared from circulation by the same pathways as FIXa, though the possibility of either of the two elimination mechanisms recognizing this intermediate would help explain the low observed *in vivo* recovery of tg-FIX.

The plasma concentration versus time profiles of tg-FIX and pd-FIX were evaluated by three pharmacokinetic techniques: one and two-compartmental models and a model-independent analysis. All three techniques yielded similar values for the circulation half-lives for both pd-FIX and tg-FIX, as shown in Figure 5-5. This agreement occurs despite differences in the how well the concentration versus time data

was fit by the one and two-compartment models, with the two-compartmental bi-exponential equation yielding a better fit of the data. However, due to the low number of data points, especially very early after injection where the distribution term is most important, the improvement in the fit was found not to be statistically significant given the introduction of two additional fitted parameters for the bi-exponential equation. As a result, given the data from this study, the more simplistic one-compartment model was determined to be the most likely representation of the behavior of FIX in the mouse model experiments performed here.

Pharmacokinetic Method	**tg-FIX $t_{1/2}$ (hr)**	**pd-FIX $t_{1/2}$ (hr)**
One-compartment model	27.0	16.0
Two-compartment model	28.0	13.8
Non-compartmental (Average)	26.5	13.2

Table 5-5. Summary of the circulation half-lives of tg-FIX and pd-FIX calculated by compartmental and non-compartmental methods. The reported two-compartment model half-life is the $t_{1/2elim}$. The non-compartmental values represent the average of both the analytical and numerical integrations of the MRT function.

From this analysis, it can bee seen that the circulation half-life of tg-FIX is roughly twice that observed for pd-FIX. Because the primary amino acid sequence as determined by the encoding FIX transgene should be identical, this extended half-life is most likely related to the altered PTM profile of tg-FIX compared to pd-FIX. Because FIX is so heavily post-translationally modified, any number of PTMs could have an effect on the observed difference, including the presence and structure of N or O-linked glycans, phosphorylation, sulfation, and Gla content.

Preliminary PTM analysis was performed to determine if tg-FIX is N-glycosylated or phosphorylated similarly to pd-FIX. It was found that tg-FIX, identically to pd-FIX, contains N-linked oligosaccharides on the activation peptide capable of being excised by PNGase. PNGase digestions do not yield any detailed information about the structure of these glycans, however. Data has been collected describing the sialic acid content of tg-FIX, which has been shown to be slightly lower to that recorded for pd-

FIX[kvc1] (GC Gil, personal communication, December 2, 2004). Additionally, published reports indicate that the porcine mammary gland can produce a complex-type glycosylation pattern similar to that found in human glycoproteins without the formation of high-mannose structures,[35] which has been confirmed by additional experiments for tg-FIX (unpublished results). Together, these results indicate that tg-FIX likely is not susceptible to known N-linked glycan-related clearance mechanisms. Additionally, it was found that tg-FIX exhibits a phosphorylation pattern similar to pd-FIX, representing a more wild-type PTM structure than CHO cell rFIX, likely eliminating this PTM as a cause of the altered pharmacokinetics.

FIX in circulation distributes between the plasma and the endothelium through interactions of the FIX Gla domain with collagen IV.[36,37] Formation of the FIX endothelial cell binding site is dependent upon the Ca^{2+}-induced structure of the FIX Gla domain and specifically involves amino acids 3-11, including Gla residues at positions 7 and 8.[38] Amino acid analysis revealed that tg-FIX contains an average 7 of the 12 carboxylations found in pd-FIX. Because tg-FIX possesses a non-native Gla domain, it is possible that interaction between these molecules and the endothelium differs from pd-FIX with a fully carboxylated Gla domain. Experimentally, the endothelial cell binding characteristics of the FIX Gla domain have been found to affect the rate of FIX clearance and subsequently its circulation half-life. Gui et al. (2002)[24] discovered that two Gla domain mutants that display altered endothelial cell binding properties also possess altered pharmacokinetic profiles. A FIX mutant with high affinity for endothelial cells was shown to possess an extended circulation half-life. This mutant was characterized by rapid initial elimination from plasma followed by slow clearance over time. Conversely, an endothelial cell non-binding FIX mutant was characterized by a shorter circulation half-life. This mutant did not experience rapid initial elimination from plasma, but instead was cleared at an increased rate throughout its circulation. The hypothesized cause for the difference in pharmacokinetic profiles is the transient translocation of FIX from plasma to the endothelium. The stronger the interaction between a FIX population and the endothelium, the larger the percentage of that FIX population that is sequestered to the endothelium and the more slowly it is released back into plasma. In this way, the

endothelium can be thought of as a FIX reservoir in which it is protected from the normal clearance mechanisms.

It is not known if either of the two Gla residues directly associated with endothelial cell binding are carboxylated in the active tg-FIX isoforms. However, since the coordination of individual Ca^{2+} ions in the Gla domain occurs through multiple Gla residues, the endothelial cell binding site may be transformed even if the missing carboxylations are not present in the binding site itself. For example, Gla's 27, 17, and 7 all interact with a single Ca^{2+} ion, with only Gla 7 directly associated with the endothelial binding site.[39] Consequently, if any of these three glutamic acid residues are not carboxylated, the structure of the endothelial cell binding site may be altered. As a result, it seems very likely that the elimination of 5 carboxylations in FIX would have some effect on the interaction of tg-FIX with the endothelium, though the nature of this effect, either strengthening or weakening, is difficult to predict. If tg-FIX associates with the endothelium with a higher affinity, this could explain the increase in half-life experienced by tg-FIX. Additionally, stronger endothelial cell binding properties could be another cause of the observed low recovery since a larger percentage of tg-FIX than pd-FIX would be translocated out of plasma to the vascular walls immediately after injection. The reduced redistribution rate constant, k_{21}, calculated in the two-compartment model for tg-FIX lends credence to this hypothesis.

It should be pointed out that the tg-FIX preparation used in this study is most likely not composed of homogeneous FIX containing exactly 7 Gla residues. It was shown that the injected tg-FIX exists as a mixture of proteolytic products and additionally, as shown in Chapter 4, a small percentage (~10%) of this tg-FIX likely still contains the propeptide. As a result, it is possible that the observed pharmacokinetic profile for tg-FIX is a result of the sum of FIX isoforms, each with its own pharmacokinetic properties. For example, one population of tg-FIX may contain 6 Gla residues while another may contain 7 and yet another may contain 8. Each of these FIX isoforms, for instance, may possess unique endothelial cell binding affinities, thus possess different circulating properties. For the purposes of this study, however, evaluation of the pharmacokinetic properties of tg-FIX were performed as if it represented a homogenous population. This

fact, however, does not diminish the results from this study, as even the current rFIX product, BeneFIX®, has been shown to be comprised of a mixture of PTM isoforms.[40]

5.5 Summary and Future Work

In this research, a tg-FIX product derived from transgenic pig milk was produced and its pharmacokinetic behavior *in vivo* in FIX gene-knockout mice was studied. Compared to pd-FIX, tg-FIX was characterized by lower recovery, approximately one-sixth, and an extended circulation half-life, 27 hours for tg-FIX compared to 16 hours for pd-FIX as calculated from the one-compartment pharmacokinetic model. These altered pharmacokinetic properties are most likely a result of differences in the extent and nature of proteolytic and post-translational processing of tg-FIX. It was shown that a large percentage of the tg-FIX used in this study is proteolyzed to FIXa and FIXα, yielding FIX species potentially susceptible to rapid inactivation and clearance *in vivo*. Tg-FIX was shown to possess similar phosphorylation and N-linked glycosylation but a reduced Gla content compared to pd-FIX. It was hypothesized that the extended circulation half-life and low recovery of tg-FIX could be the result of altered endothelial cell binding properties resulting from a non-native tg-FIX Gla domain. Importantly tg-FIX retains its clotting activity, despite containing an average of only 7 Gla residues. These results suggest that tg-FIX has the potential to provide an efficacious alternate source of FIX for hemophilia B therapy, and that these molecules *may*, in fact, possess advantageous pharmacokinetic properties. A FIX product with an extended circulation half-life has been the goal of FIX researchers for many years as it would result in a reduction of the frequency of injections required to maintain circulating FIX levels in prophylaxis. However, this study represents only a first step in characterizing the pharmacokinetic properties of active tg-FIX. Several questions were raised during the course of this work, and in order to fully describe the pharmacokinetics of tg-FIX, more investigation is required.

It was proposed that the low *in vivo* recovery of FIX could be explained in large part by rapid elimination of FIXa and FIXα from plasma by the ATIII and LRP pathways. This hypothesis can be tested simply by eliminating these activation products from the

injected tg-FIX preparation and comparing recoveries. A chromatographic process for selectively purifying FIXa is currently being investigated. Despite similar primary amino acid sequence, structural elements in the heavy chain, including the active site and heparin binding site,[41,42] and activation peptide that differ between zymogen FIX, FIXa, and FIXα may lend themselves to be a means for separation. To obviate the necessity of such a purification process, however, transgenic pig milk that contains a much lower initial level of FIXa and FIXα has been identified. Using this milk as a feedstock, a tg-FIX product has been generated in which the large majority of tg-FIX exists as single-chain zymogen.

Future pharmacokinetic experiments should be performed to unequivocally determine if tg-FIX possess an extended circulation half-life compared to pd-FIX. Two factors limited the analysis presented here: 1) the presence of FIXa and FIXα in the injected tg-FIX preparation and 2) the limited number of collected data points. As mentioned above, a tg-FIX product devoid of FIXa and FIXα, as well as any proFIX, has been generated (see Chapter 4, Figure 4-3). This material is more homogeneous and its use would eliminate one of the potential causes of the altered tg-FIX pharmacokinetics. Moreover, to aid in the mathematical analysis, additional data points should be collected over the course of the experiment. Of special interest are times immediately after injection so that the often observed distribution phase of FIX pharmacokinetics can be resolved. Taking several points from 2 to 15 minutes post-injection would be of great vale in characterizing the normally observed biphasic nature of FIX pharmacokinetics. Taking timepoints between 4 and 48 hours post-injection would also be beneficial in order to better characterize the elimination half-life values.

If the pharmacokinetics experiments described above confirm the findings of this study, additional experiments need to be directed at unequivocally determining the cause of the extended tg-FIX half-life. It was hypothesized that the prolonged circulation half-life of tg-FIX is most likely a consequence of its altered post-translational processing, more specifically a result of the lower level of γ-carboxylation of tg-FIX. The proposed hypothesis was that the extended half-life of tg-FIX could be a byproduct of high endothelial cell binding affinity derived from its reduced Gla content. This hypothesis could readily be tested through endothelial cell binding studies. The method described by

Cheung et al.[36] for determination of endothelial cell binding strength of radiolabled FIX could be adapted for use with tg-FIX. By quantitative comparison of the endothelial cell binding strength of tg-FIX and pd-FIX, a clearer understanding of the mechanism of tg-FIX half-life extension could be achieved. By analogy to the results of Gui et al.,[24] an observed higher binding strength for tg-FIX would likely be the cause of the extended half-life and contribute to its low recovery. However, if it was determined that tg-FIX possessed similar or lower affinity for endothelial cells, an alternate explanation for the extended circulation half-life, perhaps a result of differences in the other FIX PTMs, would need to be derived.

As a result, further investigation of the tg-FIX PTMs would be of great value in characterizing the tg-FIX pharmacokinetic profile. In depth N-linked glycan structure analysis is currently underway and future work determining the extent of tyrosine sulfation, perhaps through mass spectroscopy, should to be undertaken. Preliminary phosphorylation analysis presented in this work indicated that tg-FIX is likely phosphorylated on the activation peptide identically to pd-FIX, eliminating this PTM as a probable cause of the altered pharmacokinetics. Tg-FIX may provide a unique opportunity to study the effects of these PTMs on the FIX circulating characteristics by exploiting natural differences in PTM profile compared to pd-FIX that arise through the use of the transgenic pig bioreactor. Through these experiments, information useful for both a more detailed understanding of the mechanisms of FIX clearance *in vivo* as well as for future design of recombinant FIX products with more beneficial pharmacokinetic properties could be obtained.

---

[1] Ewenstein BM, Joist JH, Shapiro A, Hofstra TC, Leissinger CA, Seremetis SV, Broder M, Mueller-Velten G, Schwartz BA. 2002. Pharmacokinetic analysis of plasma-derived and recombinant FIX concentrates in previously treated patients with moderate or severe hemophilia B. *Transfusion* 42: 190-197.

[2] Heimark R, Schwartz SM. 1983. Binding of coagulation factors IX and X to the endothelial cell surface. *Biochm Biophys Res Commun* 111: 723-731.

[3] Stern DM, Drillings M, Nossel HJ, Hurlet-Jensen A, LaGamma KS, Owen J. 1983. Binding of factors IX and IXa to cultured vascular endothelial cells. *Proc Natl Acad Sci USA* 80: 4110-4123.

[4] Fuchs HE, Trapp HG, Griffith MJ, Roberts HR, Pizzo SV. 1984. Regulation of factor IXa in vitro in human and mouse plasma and in vivo in the mouse: Role of the endothelium and the plasma proteinase inhibitors. *J Clin Invest* 73: 1696-1703.

[5] Sheffield WP, Mamdani A, Hortelano G, Gataiance S, Eltringham-Smith L, Begbie ME, Leyva RA, Liaw PS, Ofosu FA. 2004. Effects of genetic fusion of factor IX to albumin on in vivo clearance in mice and rabbits. *Brit J Haematol* 126: 565-573.

[6] Kaufman RJ. 1998. Post-translational modifications required for coagulation factor secretion and function. *Thromb Haemostasis* 79: 1068-1079.

[7] White G, Shapiro A, Ragni M, Garzone P, Goodfellow J, Turbidity K, Courter S. 1998. Clinical evaluation of recombinant factor IX. *Seminars Hematol* 35(Suppl. 2): 33-38.

[8] Arruda VR, Hagstrom JN, Deitch J, Heiman-Patterson T, Camire RM, Chu K, Fileds PA, Herzog RW, Couto LB, Larson PJ, High KA. Post-translational modifications of recombinant myotube-synthesized human factor XI. 2001. *Blood* 97: 130-138.

[9] White GC, Beebe A, Nielsen B. 1997. Recombinant factor IX. *Thromb Haemostasis* 78: 261-265.

[10] Ashwell G, Morell AG. 1974. The role of surface carbohydrates in the hepatic recognition and transport of circulating glycoproteins. *Adv Enzymol Relat Areas in Mol Biol* 41: 99-128.

[11] Gerngross TU. 2004. Advances in the production of human therapeutic proteins in yeasts and filamentous fungi. *Nature Biotech* 22: 1409-1414.

[12] Lin HF, Maeda N, Smithies O, Straight DL, Stafford DW. 1997. A coagulation factor IX-deficient mouse model for human hemophilia B. *Blood* 90: 3962-3966.

[13] Kung SH, Hagstrom JN, Cass D, Tai SJ, Lin HF, Stafford DW, High KA. 1998. Human factor IX corrects the bleeding diathesis of mice with hemophilia B. *Blood* 91: 784-790.

[14] Chao H, Monahan PE, Liu Y, Samulski RJ, Walsh CE. 2001. Sustained and complete phenotype correction of hemophilia B mice following intramuscular injection of AAV1 serotype vectors. *Mol Ther* 4: 217-222.

[15] Lin HF, Maeda N, Smithies O, Straight DL, Stafford DW. 1997. A coagulation factor IX-deficient mouse model for human hemophilia B. *Blood* 90: 3962-3966.

[16] Kung SH, Hagstrom JN, Cass D, Tai SJ, Lin HF, Stafford DW, High KA. 1998. Human factor IX corrects the bleeding diathesis of mice with hemophilia B. *Blood* 91: 784-790.

[17] Chao H, Monahan PE, Liu Y, Samulski RJ, Walsh CE. 2001. Sustained and complete phenotype correction of hemophilia B mice following intramuscular injection of AAV1 serotype vectors. *Mol Ther* 4: 217-222.

[18] Lindsay M, Gil GC, Cadiz A, Velander WH, Zhang C, Van Cott KE. 2004. Purification of recombinant DNA-derived factor IX produced in transgenic pig milk and fractionation of active and inactive subpopulations. *J Chromatogr A* 1026: 149-157.

[19] Jin DY, Zhang TP, Gui T, Stafford DW. 2004. Creation of a mouse expressing defective human factor IX. *Blood* 104:1733-1739.

[20] Riviere JE. 1999.*Comparative Pharmacokinetics: Principles, Techniques, and Applications*. Iowa State University Press, Ames, IA.

[21] Morfini M. 2003. Pharmacokinetics of factor VIII and factor IX. *Haemophilia* 9: 94-100/

[22] Usansky JI, Desai A, Tang-Liu D. PK functions for Microsoft Excel. Available on the internet at: www.boomer.org/software

[23] Bjorkman S, Shapiro AD, Berntorp E. 2001. Pharmacokinetics of recombinant factor IX in relation to age of the patient: implications for dosing and prophylaxis. *Haemophilia* 7: 133-139.

[24] Gui T, Lin JF, Jin DY, Hoffman M, Straight DL, Roberts, Stafford DW. 2002. Circulating and binding characteristics of wild-type factor IX and certain Gla domain mutants in vivo. *Blood* 100: 153-158.

[25] Berntorp E, Bjorkman S, Carlsson M, Lethagen S, Nilsoon IM. 1993. Biochemical and in vivo properties of high purity factor IX concentrates. *Thromb Haemostasis* 70: 768-773.

[26] Bjorkman S, Carlsson M, Bertorp E. 2001. Pharmacokinetics of factor IX in patients with hemophlia B. Methodological aspects and physiological interpretation. *Eur J Clin Pharmacol* 46: 325-332.

[27] Kurachi K, Davie EW. 1982. Isolation and characterization of a cDNA coding for human factor IX. *Proc Natl Acad Sci USA* 79: 6461-6464.

[28] Maley F, Trimble RB, Tarentino AL, Plummer TH. 1989. Characterization of glycoproteins and their associated oligosaccharides through the use of endoglycosidases. *Anal Biochem* 180: 195-204.

[29] White GC, Beebe A, Nielsen B. 1997. Recombinant factor IX. *Thromb Haemostasis* 78: 261-265.

[30] Neels JG, van den Berg BMM , Mertens K, ter Maat H, Pannekoek H, van Zonneveld AJ, Lenting PJ. 2000. Activation of factor IX zymogen results in exposure of a binding site for low-density lipoprotein receptor-related protein. *Blood* 96: 3459-3465.

[31] Moestrup SK, Gliemann J, Pallesen G. 1992. Distribution of the alpha 2-macroglobin receptor/low density lipoprotein receptor-related protein in human tissues. *Cell Tissue Res* 259:375-382.

[32] Lenting PJ, Neels JG, van den Berg BMM. Clijsters PFM, Meijerman DWE, Pannekoek H, van Mourik JA, Mertens K, van Zonneveld AJ. 1999. The light chain of factor VIII comprises a binding site for low density lipoprotein receptor-related protein. *J Biol Chem* 274: 31305-31311.

[33] Lenting PJ, ter Maat H, Clijsters PPFM, Donath MJSJ, van Mourik JA, Mertens K. 1995. Cleavage at argininte 145 in human blood coagulation factor IX converts the zymogen into a factor VIII binding enzyme. *J Biol Chem* 270: 14884-14890.

[34] Rohlena J, KolkMan JA, Boertjest RC, Mertens K, Lenting PJ. 2003. Residues Phe342-Asn346 of activated coagulation factor IX contribute to the interaction with low density lipoprotein receptor-related protein. *J Biol Chem* 278: 9394-9401.

[35] Spik G, Coddeville B, Mazurier J, Bourne Y, Cambilaut C, Montreuil J. 1994. Primary and three-dimensional structure of lactotransferrin (lactoferrin) glycans. *Adv Exp Med Biol* 357: 21-32.

[36] Cheung WF, Hamaguchi N, Smith KJ, Stafford DW. 1992. Identification of the endothelial cell binding stie for factor IX. *Proc Natl Acad Sci USA* 92: 11068-11073.

[37] Wolberg AS, Stafford DW, Erie DA. 1997. Human factor IX binds to specific sites on the collagenous domain of collagen IV. *J Biol Chem* 272: 16717-16720.

[38] Cheung WF, Hamaguchi N, Smith KJ, Stafford DW. 1992. The binding of human factor IX to endothelial cells is mediated by residues 3-11. *J Biol Chem* 267: 20529-20531.

[39] Freedman SJ, Furie BC, Furie B, Baleja JD. 1995. Structure of the calcium ion-bound γ-carboxyglutamic acid-rich domain of factor IX. *Biochemistry* 34: 12126-12137.

[40] Bond M, Jankowski M, Patel J, Karnik S, Strang A, Xu B, Rouse J, Koza S, Letwin B, Steckert J, Amphlett G, Scoble H. 1998. Biochemical characterization of recombinant factor IX. *Semin Hematol* 35: 11-17.

[41] Perera L, Darden TA, Pedersen LG. 2001. Modeling human zymogen factor IX. *Thromb Haemostasis* 88: 596-603.

[42] Yang L, Manithody C, Rezaie AR. 2002. Localization of the heparin binding exosite of factor IXa. *J Biol Chem* 277: 50756-50760.

Chapter 5: Additional Calculations

I. Two-compartment pharmacokinetic model: Two-term exponential equation fit to data

A. Calculations for pd-FIX

Vectors of pd-FIX plasma concentration versus time to be analyzed

$$\text{time} := \begin{pmatrix} 15 \\ 60 \\ 240 \\ 2880 \\ 4320 \end{pmatrix} \qquad C_{pM9data} := \begin{pmatrix} 0.63 \\ 0.59 \\ 0.51 \\ .046 \\ .035 \end{pmatrix}$$

Definition of the equation to fit the data. The first element contains the function that will approximate the data and the others contain the partial derivatives.

$$F(t,a) := \begin{bmatrix} a_0 \cdot e^{-a_1 \cdot t} + a_2 \cdot e^{-a_3 \cdot t} \\ e^{-a_1 \cdot t} \\ a_0 \cdot (-t) \cdot e^{-a_1 \cdot t} \\ e^{-a_3 \cdot t} \\ a_2 \cdot (-t) \cdot e^{-a_3 \cdot t} \end{bmatrix}$$

This vector contains guess values for the parameters a_0, a_1, a_2, and a_3

$$vg := \begin{pmatrix} .5 \\ .1 \\ .5 \\ .001 \end{pmatrix}$$

$$P := \text{genfit}(\text{time}, C_{pM9data}, vg, F)$$

This vector P contains optimal values for the parameters a_0, a_1, a_2, and a_3 as computed by the genfit function

$$P = \begin{pmatrix} 0.42 \\ 0.218 \\ 0.622 \\ 8.397 \times 10^{-4} \end{pmatrix}$$

$P_0 = 0.42$

$P_1 = 0.218$

$P_2 = 0.622$

$P_3 = 8.397 \times 10^{-4}$

Functional fit to data:

$t := (0, 10 .. 4320)$

$$C_{pM9_t} := P_0 \cdot e^{-P_1 \cdot t} + P_2 \cdot e^{-P_3 \cdot t}$$

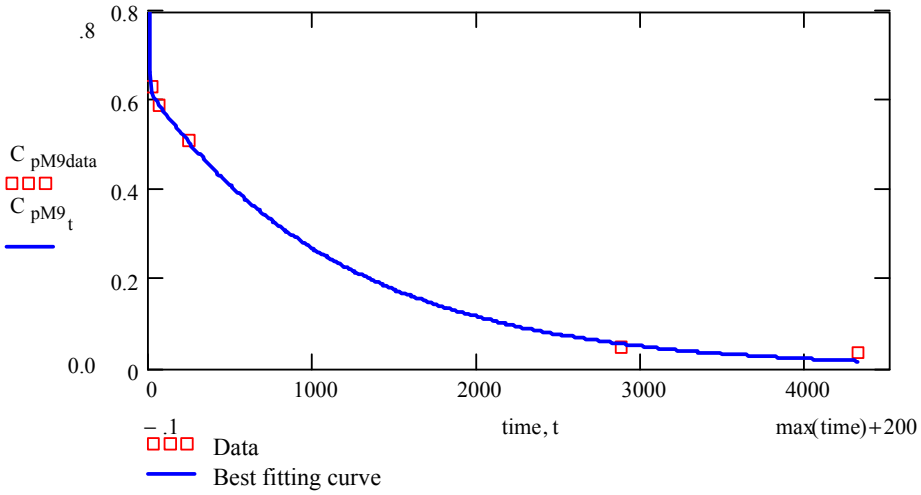

Plot of the residuals between data and fit:

$$C_{pM9}(time) := P_0 \cdot e^{-P_1 \cdot time} + P_2 \cdot e^{-P_3 \cdot time}$$

$$C_{pM9}(time) = \begin{pmatrix} 0.63 \\ 0.591 \\ 0.508 \\ 0.055 \\ 0.017 \end{pmatrix} \qquad C_{pM9data} = \begin{pmatrix} 0.63 \\ 0.59 \\ 0.51 \\ 0.046 \\ 0.035 \end{pmatrix}$$

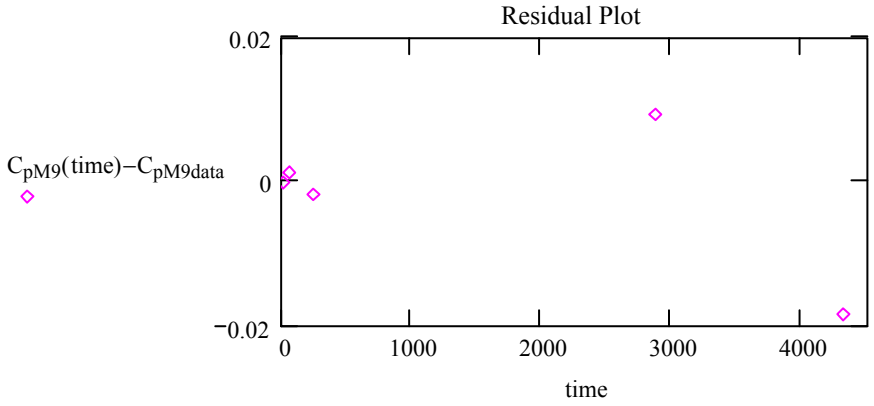

B. Calculations for tg-FIX

Vectors of pd-FIX plasma concentration versus time to be analyzed

$$\text{time} := \begin{pmatrix} 15 \\ 60 \\ 240 \\ 2880 \\ 4320 \end{pmatrix} \qquad C_{pTGdata} := \begin{pmatrix} 0.33 \\ 0.21 \\ 0.20 \\ .06 \\ .043 \end{pmatrix}$$

Definition of the equation to fit the data. The first element contains the function that will approximate the data and the others contain the partial derivatives.

$$F(t,a) := \begin{bmatrix} a_0 \cdot e^{-a_1 \cdot t} + a_2 \cdot e^{-a_3 \cdot t} \\ e^{-a_1 \cdot t} \\ a_0 \cdot (-t) \cdot e^{-a_1 \cdot t} \\ e^{-a_3 \cdot t} \\ a_2 \cdot (-t) \cdot e^{-a_3 \cdot t} \end{bmatrix}$$

This vector contains guess values for the parameters a_0, a_1, a_2, and a_3

$$vg := \begin{pmatrix} 0.3 \\ .001 \\ 0.1 \\ .001 \end{pmatrix}$$

$$P := \text{genfit}(\text{time}, C_{pTGdata}, vg, F)$$

This vector P contains optimal values for the parameters a_0, a_1, a_2, and a_3 as computed by the genfit function.

$$P = \begin{pmatrix} 0.708 \\ 0.122 \\ 0.217 \\ 4.131 \times 10^{-4} \end{pmatrix}$$

$$P_0 = 0.708$$

$$P_1 = 0.122$$

$$P_2 = 0.217$$

$$P_3 = 4.131 \times 10^{-4}$$

Functional fit to data

$t := (0, 10 .. 4320)$

$C_{pTG_t} := P_0 \cdot e^{-P_1 \cdot t} + P_2 \cdot e^{-P_3 \cdot t}$

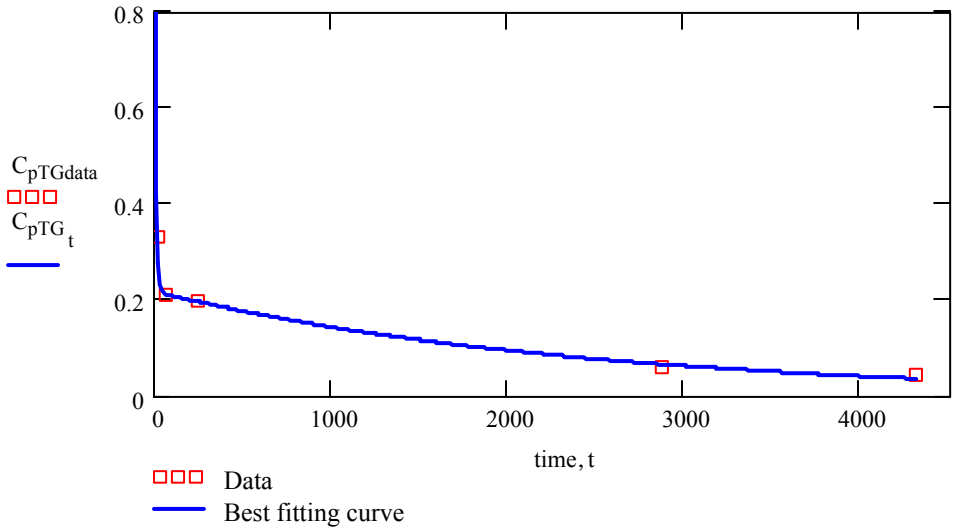

Plot of the residuals between data and fit

$C_{pTG}(time) := P_0 \cdot e^{-P_1 \cdot time} + P_2 \cdot e^{-P_3 \cdot time}$

$$C_{pTG}(time) = \begin{pmatrix} 0.33 \\ 0.212 \\ 0.197 \\ 0.066 \\ 0.036 \end{pmatrix} \qquad C_{pTGdata} = \begin{pmatrix} 0.33 \\ 0.21 \\ 0.2 \\ 0.06 \\ 0.043 \end{pmatrix}$$

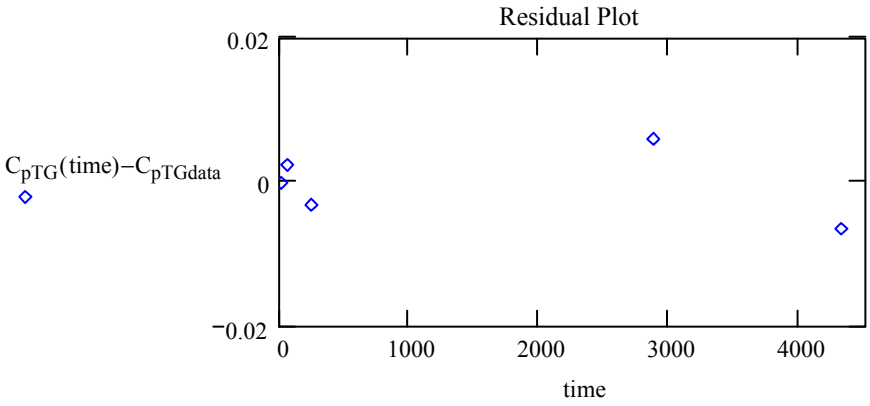

II. Non-compartmental method calculations

A. Mathcad calculation of MRT by integration of the one-term exponential equation.

$$C_{pTG_t} := 0.24477e^{-0.000428 \cdot t} \qquad C_{pM9_t} := 0.59108e^{-0.000725 \cdot t}$$

For tg-FIX

$$MRT_{TG} := \frac{\int_0^{\infty} 0.24477e^{-0.000428 \cdot t} \cdot t \, dt}{\int_0^{\infty} 0.24477e^{-0.000428 \cdot t} \, dt}$$

MRT_{TG} = 38.9 hours

For pd-FIX

$$MRT_{M9} := \frac{\int_0^{\infty} 0.59108e^{-0.000725 \cdot t} \cdot t \, dt}{\int_0^{\infty} 0.59108e^{-0.000725 \cdot t} \, dt}$$

MRT_{M9} = 23.0 hours

B. Mathcad calculation of MRT by integration of the two-term exponential fit to data.

For **pd-FIX:**

$$P_0 = 0.42$$

$$P_1 = 0.218$$

$$P_2 = 0.622$$

$$P_3 = 8.397\times 10^{-4}$$

$$AUCM9 := \int_0^{\infty} P_0\cdot e^{-P_1\cdot t} + P_2 e^{-P_3\cdot t}\, dt \qquad AUCM9 = 742.277$$

$$AUMCM9 := \int_0^{\infty} \left(P_0\cdot e^{-P_1\cdot t} + P_2\cdot e^{-P_3\cdot t}\right)\cdot t\, dt \qquad AUMCM9 = 8.817\times 10^{5}$$

$$MRT := \frac{AUMCM9}{AUCM9}\ \text{min} \qquad MRT = 1.188\times 10^{3}\ \text{min}$$

For **tg-FIX:**

$$P_0 = 0.708$$

$$P_1 = 0.122$$

$$P_2 = 0.217$$

$$P_3 = 4.131\times 10^{-4}$$

$$AUCTG := \int_0^{\infty} P_0\cdot e^{-P_1\cdot t} + P_2 e^{-P_3\cdot t}\, dt \qquad AUCTG = 531.504$$

$$AUMCTG := \int_0^{\infty} \left(P_0\cdot e^{-P_1\cdot t} + P_2\cdot e^{-P_3\cdot t}\right)\cdot t\, dt \qquad AUMCTG = 1.273\times 10^{6}$$

$$MRT := \frac{AUMCTG}{AUCTG}\ \text{min} \qquad MRT = 2.394\times 10^{3}\ \text{min}$$

C. Trapezoidal rule calculation of MRT in Microsoft Excel

Analysis by PK Functions for Microsoft Excel		
	tg-FIX	**pd-FIX**
1st order elimination rate const [1/min]	4.3E-04	7.2E-04
Half-life [min]	1601.9	957.3
Half-life [hrs]	26.7	16.0
AUC time 0 to 72 hrs (trapezoid rule)	466.4	918.7
AUC time 0 to infinity (trapezoid rule)	565.8	967.0
AUMC time 0 to 72 hrs (trapezoid rule)	555468.1	555902.3
AUMC time 0 to infinity (trapezoid rule)	1214428.5	831490.4
MRT time 0 to 72 hrs (trapezoid rule) [min]	1190.9	605.1
MRT time 0 to 72 hrs (trapezoid rule) [hrs]	19.8	10.1
MRT time 0 to infinity (trapezoid rule) [min]	2146.4	859.8
MRT time 0 to infinity (trapezoid rule) [hrs]	35.8	14.3